with ether. The extract was washed once with water and evaporated. The residue was dissolved in 0.1 mL of *i*-PrOH and analyzed by HPLC. Comparison with HPLC generated standard curves using pure **16** and **15** showed that the ratio of **16** to **15** was 55/45.

The cholesterol oleate hydrolysis experiments were performed as above, using 50-μL aliquots of a solution of cholesterol oleate (2.350 mg) dissolved in 0.58 mL of *i*-PrOH. After 60 min at 37 °C, the mixture was thoroughly extracted with CH_2Cl_2 (ether is not suitable owing to the presence of traces of peroxides). The extract was washed with water and evaporated. The residue was homogenized in an *i*-PrOH–water (1/1) solution (0.1 mL). Free cholesterol was then determined by using the cholesterol oxidase enzyme method described below. The ratio of cholesterol oleate to cholesterol was 60/40.

Cholesterol Oxidase Procedure. The reagent solution was made up by combining sodium cholate (64.5 mg), 4-aminoantipyrine (8.5 mg), phenol (61,5 mg), Na_2HPO_4 (355 mg), NaH_2PO_4 (335 mg), Carbowax 6000 (51 mL), cholesterol oxidase (EC 1.1.3.6) (5.85 units), and horseradish peroxidase (3350 units) in water (50 mL) as described by Allain et al.[40] A 10 × 10 × 30 mm cuvette was charged with 2.4 mL of the reagent solution (~37 °C) followed by 0.3 mL of *i*-PrOH (~37 °C) to which had been added either 0, 5, 10, 30, 50, or 60 μL of stock substrate solution (3.0 mg of substrate in 1.0 mL of *i*-PrOH). After the solution was mixed (37 °C), the absorbance at 500 nm due to the formation of the chromogen was monitored until a constant value was observed. Cholesterol required 15–25 min. Reactions involving nitroxide **15** required up to 90 min. A linear response was obtained for cholesterol; 5 μL gave A_{500} = 0.12; 10 μL, 0.24; 30 μL, 0.76; 60 μL, 1.58. With **15**, the maximum absorbance at 500 nm approached a limiting value: 5 μL gave A_{500} = 0.03; 10 μL, 0.14; 30 μL, 0.22; 50 μL, 0.25. The oxidation studies with **15** were complicated by formation of suspensions or fine precipitates. Another set of experiments were performed in which the concentrations of both cholesterol oxidase and horseradish peroxidase were increased 110-fold. Cholesterol behaved normally, with 30 μL of stock solution giving A_{500} = 0.78. Nitroxide **15** behaved as follows: 10 μL gave A_{500} = 0.12; 30 μL, 0.18; 50 μL, 0.35 (cloudy).

Synthesis of Tritium-Labeled Cholesterol Nitroxide 20. To a cooled suspension of *N*-chlorosuccinimide (7 mg) in 0.2 mL of dry toluene at −15 °C (N_2) was added 70 μL of a 1 M dimethyl sulfide solution in toluene. Then a solution of **15** (5 mg) in 1.0 mL of dry toluene was added dropwise, After a 2-h stir at −23 °C, 52 μL of 1 M triethylamine in toluene was added at −23 °C. The cooling bath was removed, and after 5 min, ether (15 mL) was added. The organic layer was washed with cold water and brine and dried ($MgSO_4$). After removal of solvent, **19** (5.5 mg) was obtained as a solid: mp 156–160 °C; IR ($CHCl_3$) 1710 cm^{-1}. This was used immediately for the following reduction. Sodium boro[^{3}H]hydride (100 mCi) (Amersham, sp act., ~5 Ci/mMol) was transferred to a centrifuge tube with the aid of some *i*-PrOH. A solution of **19** (5.5 mg) in 0.8 mL of *i*-PrOH was added. After a 1.5-h stir at 25 °C, 0.3 mL of 0.1 N NaOH and 0,1 mL of water were added, and then all was extracted with ether. The extract was washed with brine and evaporated, giving a residue which was purified by preparative TLC (hexane–ether, 3/7). Tritiated nitroxide **20** (2.5 mg) and its C-3 epimer (1.5 mg) were both isolated in pure form. After recrystallization of **20** from CH_3CN, the specific activity was 1.6 Ci/mM.

Preparation of Human High Density Lipoprotein (HDL_3) and HDL_3 Lipids. Human high density lipoprotein, HDL_3, was kindly supplied by Dr. Angelo M. Scanu[54] and stored at 4 °C in a high salt solution consisting of 98 mg of NaCl, 200 mg of NaBr, and 0.01 mL of 5% EDTA, pH 7.0, per milliliter (final density of 1.21 g/mL). Before use, HDL_3 was dialyzed against 0.15 M NaCl, 10 mM phosphate, 1 mM EDTA, pH 7.4, and adjusted to 30 mg of protein/mL by ultracentrifugation. The same buffer was used in all experimental procedures, Cholesterol nitroxide **15** was introduced into the lipoprotein particles at a molar ratio of less than one spin label per two HDL_3 via ethanolic injection of the label [1% (v/v) final ethanol concentration]. Full incorporation of nitroxide **15** required incubation for 8 h at 37 °C as monitored by ESR. Control experiments showed that the ESR spectrum of **7** in HDL_3 was not altered by the addition of 1% ethanol.

HDL_3 lipids were extracted by the method of Bligh and Dyer,[55] dried, resuspended in buffer, and centrifuged (1 h, 12000*g*) to separate the vesicles containing phospholipid and cholesterol from the floating apolar lipids. The phospholipid–cholesterol-rich fraction was reextracted, characterized by thin-layer chromatography, and stored in choloroform–methanol (4/1). Aqueous vesicles of the phospholipid–cholesterol HDL_3 lipid fraction and cholesterol nitroxide **15** were prepared by mixing 685 nmol of HDL_3 lipid phosphorus and 5.7 nmol of nitroxide **15** in chloroform–methanol (4/1) and drying the lipids under nitrogen followed by water aspiration (1 h). Buffer (40 μL) was added to the dry lipid film and the sample was vortexed. This procedure yields multilamellar vesicles with the same phospholipid to cholesterol ratio as the intact HDL_3.

Acknowledgment. This research was supported by Public Health Service Research Grants GM-24951 and GM-25698 from the National Institute of General Medical Sciences, We thank the Yamanouchi Pharamceutical Co. Ltd., Japan, for providing a sabbatical leave for T,T. We also thank Robert S, Norton for preforming some preliminary experiments,

(54) Scanu, A. *J. Lipid Res.* **1966**, *7*, 295–306.
(55) Bligh, E. G.; Dyer, W. J. *Can. J. Biochem. Physiol.* **1959**, *37*, 911–917.

Comparative NMR Studies of Cytochrome *c* and Its Active Site Octapeptide

Michele Smith and George McLendon*

Contribution from the Department of Chemistry, University of Rochester, Rochester, New York 14627. *Received November 3, 1980*

Abstract: The source of the asymmetric electron spin density distribution in cytochrome *c* has been investigated with use of the active site heme octapeptide (OP) as a model system, The paramagnetic ^{1}H NMR spectra of OPL where L = CN^-, pyridine, N_3^-, and *N*-acetyl-DL-methionine are reported and compared to the spectra of analogous cytochrome *c* derivatives. The temperature and concentration dependences of the OPCN and OPpyr heme methyl resonances were used to characterize the model system. Low-temperature EPR spectra of OPCN and OPpyr are very similar to their respective cytochrome *c* analogues. The *g* values were used to calculate the dipolar contribution to the isotropic shifts. Large isotropic shift differences between the appropriate model system and cytochrome *c* derivative primarily reflect greater contact shifts in the peptide systems, in contrast to previous model system studies. Heme methyl group resonances were assigned for OPCN, OPpyr, azide–cytochrome *c*, and pyridine–cytochrome *c*, using either Gd^{3+} as a relaxation probe or saturation transfer for N_3^- and pyridine–cytochrome *c* complexes. The pattern of methyl group resonances with increasing field presumably is 5, 8, 1, 3 for the model systems as well as for the protein derivatives, compared to 8, 3, 5, 1 for native cytochrome *c*. The detailed analysis of these results demonstrates that the orientation of the axial methionine in cytochrome *c* and heme-protein contacts are important determinants of the electronic structure of the heme in native cytochrome *c*.

NMR spectroscopy can provide a uniquely sensitive probe of the electronic structure of paramagnetic heme proteins.[1-20] This ability has been elegantly exploited in studies of cytochrome *c*, One finding of such studies is that the spin density in cytochrome

0002-7863/81/1503-4912$01.25/0

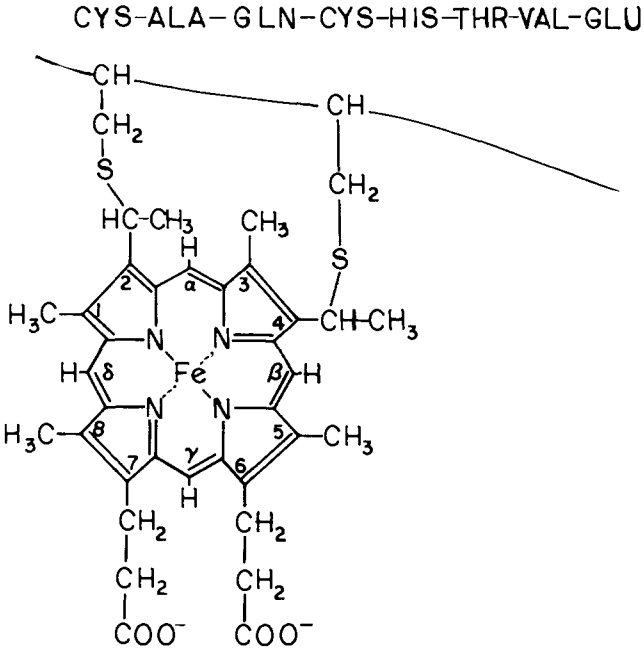

Figure 1. Schematic diagram of the cytochrome *c* heme octapeptide showing the porphyrin numbering scheme.

c appears to be anisotropically distributed,[1,2,21] with a high spin density at the exposed heme edge. Wüthrich has suggested that this electron distribution may be functionally important in electron transfer.[12,19] However, the basis for this particular distribution is unclear. Several factors could contribute to the observed anisotropy including the inequivalent heme substituents, the interaction of the heme with neighboring amino acids, and the nature and orientation of the axial ligands (methionine 80 and histidine 18 in native cyt *c*). We have sought to identify the basis for the unique electronic structure of cytochrome *c* by comparing the spin distribution of cytochrome *c* in various ligation states to that of an isolated active site peptide, the heme octapeptide first described by Harbury[22] (Figure 1). In these studies, the observed hyperfine shifts have been corrected for contact and dipolar contributions. The present studies thus help reveal how the protein interacts with heme *c* to alter the electronic structure of the heme.

Experimental Section

Materials. Horse heart cytochrome *c* (Sigma Type VI), deuterated solvents (Aldrich), and Baker Analytic Reagent KCN were used as received. Sodium azide was recrystallized from a water–ethanol mixture. Phosphate buffer was deuterated by repeated dissolution and lyophilization of the phosphate salts in D_2O. The uncorrected pH meter reading of the 0.05 M deuterated phosphate buffer was 7.1. The heme octapeptide was prepared as reported by Harbury and Loach[22] with minor modifications as described previously.[23]

Nuclear magnetic resonance spectra were obtained with either a JEOL JNM-PS-100 Fourier transform spectrometer or a WH-400 MHz Bruker spectrometer equipped with an Aspect 2000 computer system. Spectra of the octapeptide complexes taken on the 100 MHz JEOL spectrometer had spectral widths of 5K, 4–8K data points, and 200–500 scans. The residual water peak was eliminated from the spectra by using either a WEFT pulse sequence[24] or block averaging in the frequency domain accumulation mode. Spectra of cytochrome *c* derivatives were determined on a 400 MHz spectrometer with homonuclear decoupling of the residual HOD peak. Typical spectral widths of 30 kHz and 16K data points were used. 2,2-Dimethyl-2-silapentane-5-sulfonate, DSS, was used as an internal reference and downfield chemical shifts are assigned negative numbers.

Solutions of cytochrome *c* and the octapeptide were made up in 0.05 M deuterated phosphate buffer in NMR tubes capped with rubber septa. In order to investigate dimerization, octapeptide concentrations were varied between 0.01 mM and 10 mM. The cyanide and pyridine octapeptide complexes were prepared by adding concentrated solutions of ligands to NMR tubes with a gas tight microliter syringe until no further changes in the spectrum were observed and the high spin spectrum disappeared. The azide complex was prepared by adding solid sodium azide and octapeptide to the NMR tube and dissolving with the deuterated phosphate buffer and deuterated MeOH. The cyanide, pyridine, and azide derivatives of cytochrome *c* were prepared in a similar manner. Addition of the ligands was stopped when substitution of the axial methionine was complete, as evidenced by the absence of the characteristic upfield peak due to coordinated methionine.[1]

The temperature dependence of the isotropically shifted resonances for OPCN and OPpyr was determined on the JEOL spectrometer equipped with a variable temperature unit. The probe temperature was checked with either a methanol or ethylene glycol sample[25] and ranged between −3 and 36 °C.

Low-temperature EPR spectra of the cyanide and pyridine complexes of octapeptide and cytochrome *c* were obtained as frozen solutions on a X-band spectrometer at the National Biomedical EPR Center (9 K) or in Dr. W. Orme-Johnson's laboratory (13 K).

Results

Self-Association of OP. The present investigation of the magnetic properties of the heme octapeptide (OP) has also revealed the complex chemistry of OP itself. Aggregation of natural porphyrins is common[26,27] and OP is no exception.[22,28-30] Previous studies show that OP aggregation involves multiple complex equilibria.[29] Low concentrations and the addition of ligands disperse aggregates of OP.[28-30] Similar behavior was observed in the NMR and EPR spectra of OP and in ligand bonding to OP. In order to utilize the heme OP as a model system for cytochrome *c*, it is important to recognize the individual properties of the aggregates and monomers.

Concentrated solutions of free OP contain a substantial fraction of aggregates which show up in the NMR and EPR spectra. The room-temperature NMR spectrum has broad peaks (−87.6, −81.3,

(1) Wüthrich, K. *Proc. Natl. Acad. Sci. U.S.A.* **1969**, *63*, 1071–1078.
(2) Gupta, R. K.; Redfield, A. G. *Science* **1970**, *169*, 1204–1205.
(3) Morishima, I.; Ogawa, S.; Yonezawa, T.; Iizuka, T. *Biochim. Biophys. Acta* **1977**, *495*, 287–298.
(4) Miroshiam, I.; Ogawa, S.; Yonezawa, T.; Iizuka, T. *Biochim. Biophys. Acta* **1978**, *532*, 48–56.
(5) Gupta, R. K.; Redfield, A. G. *Biochem. Biophys. Res. Commun.* **1970**, *41*, 273–281.
(6) Redfield, A. G.; Gupta, R. K. *Cold Spring Harbor Symp. Quant. Biol.* **1971**, *36*, 405–411.
(7) Moore, G. R.; Williams, R. J. P. *Eur. J. Biochem.* **1980**, *103*, 513–521.
(8) Moore, G. R.; Williams, R. J. P. *Eur. J. Biochem.* **1980**, *103*, 523–532.
(9) Moore, G. R.; Williams, R. J. P. *Eur. J. Biochem.* **1980**, *103*, 533–541.
(10) Moore, G. R.; Williams, R. J. P. *Eur. J. Biochem.* **1980**, *103*, 543–550.
(11) Mayer, A.; Ogawa, S.; Shulman, R. G.; Yamane, T.; Cavaleiro, J. A. S.; d'A. Rocha Gonsalves, A. M.; Kenner, G. W.; Smith, K. M. *J. Mol. Biol.* **1974**, *86*, 749–756.
(12) Keller, R. M.; Wüthrich, K. *Biochim. Biophys. Acta* **1978**, *533*, 195–208.
(13) Moore, G. R.; Williams, R. J. P. *Eur. J. Biochem.* **1980**, *103*, 493–502.
(14) Moore, G. R.; Williams, R. J. P. *Eur. J. Biochem.* **1980**, *103*, 503–512.
(15) McDonald, C. C.; Phillips, W. D. *Biochemistry* **1973**, *12*, 3170–3186.
(16) Keller, R. M.; Pettigrew, G. W.; Wüthrich, K. *FEBS Lett.* **1973**, *36*, 151–156.
(17) Moore, G. R.; Williams, R. J. P. *FEBS Lett.* **1975**, *53*, 334–338.
(18) LaMar, G. N. In "Biological Applications of Magnetic Resonance", Shulman, R. G., ed.; Academic Press: New York, **1979**; pp 305–343.
(19) Wuthrich, K. Struct. Bonding (*Berlin*) **1970**, *8*, 53–121.
(20) Jesson, J. P. In "NMR of Paramagnetic Molecules", LaMar, G. N., Horrocks, W. D., Jr., Holm, R. H., Eds.; Academic Press: New York, 1973; Chapter 1.
(21) Shulman, R. G.; Clarum, S. H.; Karplus, M. *J. Mol. Biol.* **1971**, *57*, 93–115.
(22) Harbury, H. A.; Loach, P. A. *J. Biol. Chem.* **1960**, *235*, 3640–3646.
(23) Smith, M. C.; McLendon, G. *J. Am. Chem. Soc.* **1980**, *102*, 5566–5570.
(24) Patt, S. L.; Sykes, B. D. *J. Chem. Pshy.* **1972**, *56*, 3182–3184.
(25) VanGeet, A. L. *Anal. Chem.* **1968**, *40*, 2227–2229.
(26) White, W. J. In "The Porphyrins"; Academic Press: New York, 1979; Vol. V, Chapter 7.
(27) Caughey, W. S.; York, J. L.; Iber, P. K. In "Magnetic Resonance in Biological Systems", Ehrenberg, A., et al., Eds.; Pergamon: Oxford, 1967; p 25.
(28) Harbury, H. A.; Loach, P. A. *J. Biol. Chem.* **1960**, *235*, 3646–3653.
(29) Harbury, H. A.; Loach, P. A. *J. Biol. Chem.* **1966**, *241*, 4299–4303.
(30) Urry, D. W.; Pettegrew, J. W. *J. Am. chem. Soc.* **1967**, *89*, 5276–5283.

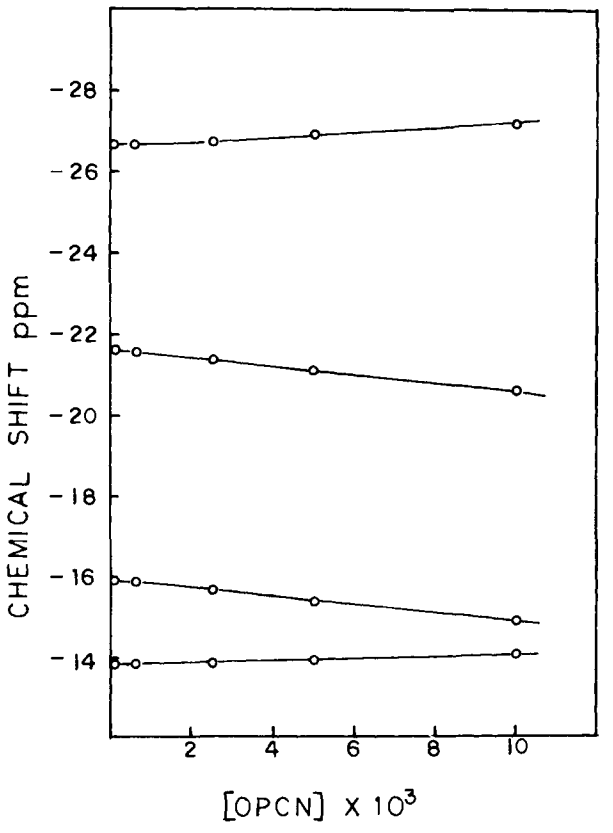

Figure 2. Concentration dependence of heme methyl shifts for OPCN.

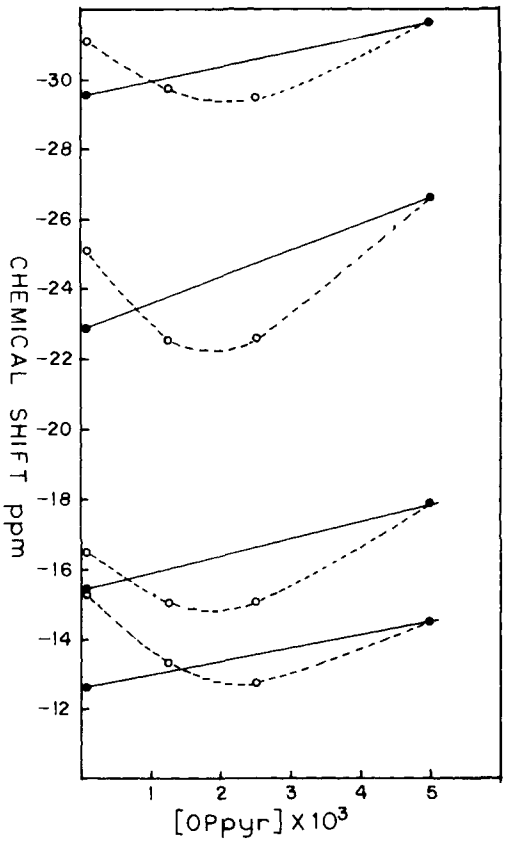

Figure 3. Concentration dependence of heme methyl shifts for OPpyr: O, constant ratio of OP/pyr; and, ●, constant excess pyridine concentration.

−71.1, −69.4 ppm from DSS) characteristic of a high-spin species,[18] presumably OP (HOD). Sharper peaks (−29.1, −27.3, −15.2, −13.3 ppm from DSS) representative of a low-spin species[18] were also visible and probably due to aggregates. The positions and relative intensities of all these peaks changed with temperature and the addition of methanol, which is indicative of a complex equilibrium between monomers and aggregates. The EPR spectrum of free OP was heterogeneous with characteristic g values (~5.9 and ~2) of high spin hemes.[31] A low-spin species with g ~3.1 and very broad hetereogeneous features around g ~2.4–2.0 and 1.8–1.4 was also present,

The cyanide OP complex exhibited concentration-dependent chemical shifts and line widths, as shown in Figure 2. The magnitude of the change in chemical shift and line width differs for each peak. This behavior again indicates self-association. The concentration dependence of OPpyr was complicated by a competing reaction, which accounts for the curvature in Figure 3, Lower concentrations of OPpyr with a constant ligand to OP ratio resulted in very broad heme methyl group peaks and methyl peaks shifting further downfield. Competing equilibria, which probably involve aggregated high-spin species, dominate the chemistry under these conditions. The equilibrium is shifted to favor the formation of monomeric OPpyr at low concentrations by increasing the concentration of pyridine. The average change of methyl group shifts was 0.7 ppm for OPCN and 2.3 ppm for OPpyr.

The self-association hinders ligand binding to OP if the ligand has a small affinity for OP. The azide and *N*-acetyl-DL-methionine OP complexes were only formed at low concentrations of OP and high concentrations of ligand. The addition of methanol to OPN_3 inhibits aggregation so a higher concentration of OPN_3 can be reached. The same methyl group peaks were observed with dilute (0.1 mM) OPN_3 samples as well as the more concentrated (1 mM) solutions containing 20% methanol. The methyl group peaks were absent in identical samples containing 20% methanol and no azide, which confirms the assignment of the peaks as methyl group resonances of OPN_3. The *N*-acetyl-DL-methionine complex was only formed at very low OP concentrations (~60 μM) due to its small formation constant (~0.5 M^{-1}) and the competition between ligation and aggregation.

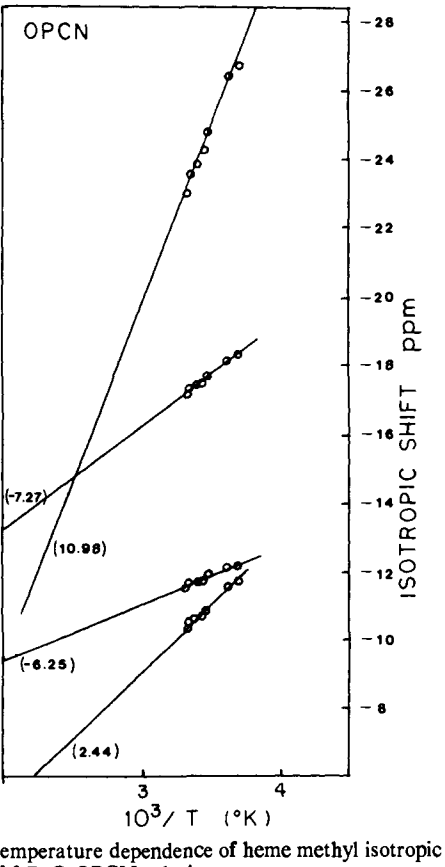

Figure 4. Temperature dependence of heme methyl isotropic shifts for an ~0.005 M D_2O OPCN solution.

(31) Peisach, J.; Blumberg, W. E.; Alder, A. *Ann. N. Y. Acad. Sci.* **1973**, *206*, 310–327.

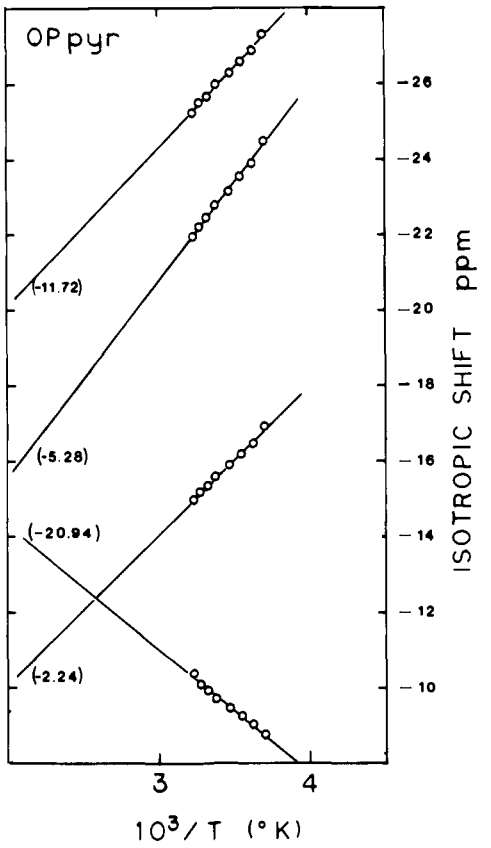

Figure 5. Temperature dependence of heme methyl isotropic shifts for an ~0.010 M D_2O OPpyr solution.

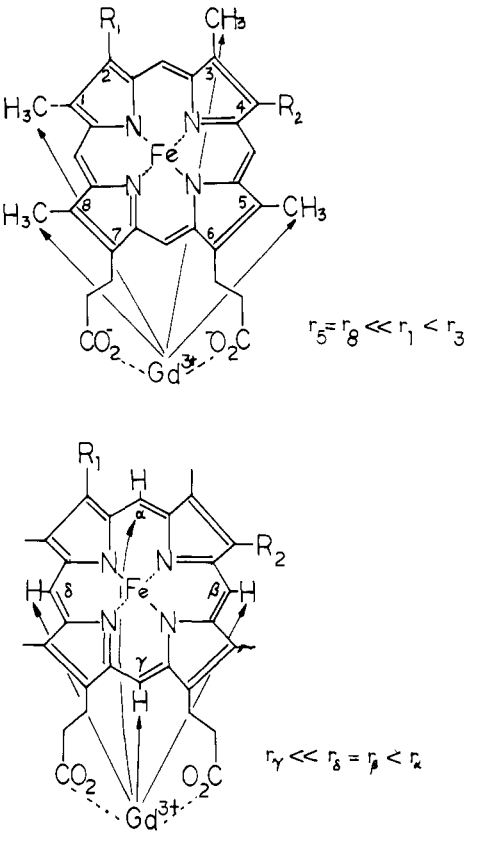

Figure 6. Coordination site of Gd^{3+} relaxation probe and relative distances of heme substituents.

Temperature Dependence. The temperature dependence of the heme methyl group isotropic shifts of OPCN and OPpyr is shown as Curie plots in Figures 4 and 5. Extrapolation of the linear region of the plot to infinitely high temperatures should pass through the origin. The actual value of the isotropic shift at $1/T = 0$ is given in parenthesis. Deviations from Curie behavior, illustrated by the non-zero intercepts, are probably mainly due to OP aggregates present at higher concentrations.[19,28-30] Other factors responsible for non-Curie behavior may include second-order Zeeman effects which have been observed in other low-spin Fe(III) heme systems.[32] The temperature dependence of OPN_o was not investigated since it is known to be in spin equilibrium.[33]

The 3-methyl group of OPpyr (vide infra) exhibits an inverted temperature dependence. Its isotropic shift increases with increasing temperature. This behavior may be due to steric interactions with the alanine–glutamine section of the peptide and the 3-methyl group. Alternatively the aggregate structure may be responsible for distorting the orientation of the 3-methyl group. As the temperature is raised the steric restriction is lessened and the contact shift increases.[34] Dominant dipolar shifts cannot be responsible for this temperature dependence since unrealistic distortions would be required for $|\theta| < 54.4°$.[35]

Assignment of OPL Methyl Groups. The methyl groups in OPCN and OPpyr were assigned by using gadolinium(III) as a relaxation probe. The Gd^{3+} apparently coordinates to the propionic side chains of the heme.[36] The paramagnetic relaxation probe shortens the spin–spin relaxation time of nearby protons through a dipolar interaction, the magnitude of which is proportional to

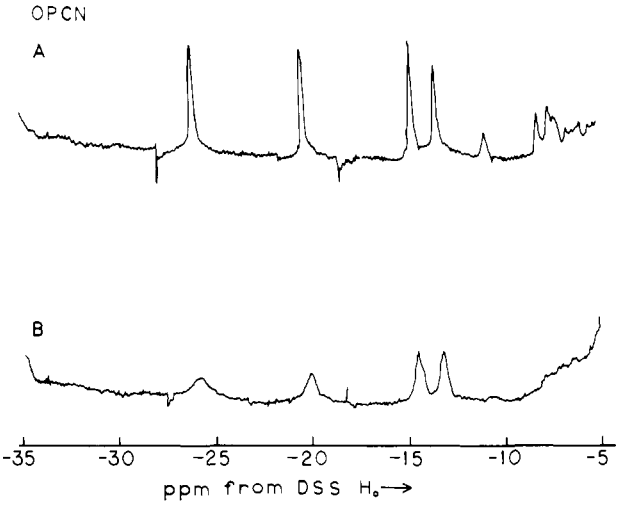

Figure 7. 100 MHz ^1H NMR spectra of ~0.005 M OPCN in D_2O at 22 °C (A) in the absence of Gd^{3+} and (B) with 5.4×10^{-4} M $GdCl_3$.

r^{-6},[20] As shown schematically in Figure 6 this method is capable of distinguishing between two of the four methyl groups in OP.

Relaxation probes used previously for assigning porphyrin resonances in noncoordinating organic solvents were inadequate for aqueous solution studies.[36,37] These cationic probes did not bind to the porphyrin due to competition between water and the propionic acid side chains for coordination sites. Gd^{3+} was used as the relaxation probe since it apparently has a greater affinity for carboxylic acids than for water, cyanide, or pyridine.

The effect of Gd^{3+} on the line widths of the methyl resonances of OPCN and OPpyr is shown in Figures 7 and 8. The resonances furthest downfield broaden out more than the two upfield peaks

(32) Horrocks, W. D., Jr.; Greenberg, E. W. *Biochim. Biophys. Acta* **1973**, *322*, 38–44.
(33) Huang, Y. P.; Kassner, R. J. *J. Am. Chem. Soc.* **1979**, *101*, 5807–5810.
(34) LaMar, G. N.; Walker, F. A. *J. Am. Chem. Soc.* **1973**, *95*, 1782–1790.
(35) Richardson, P. F. Ph.D. Dissertation, University of Rochester, 1977.
(36) Brassington, J. C.; Williams, R. J. P.; Wright, P. E. *J. Chem. Soc., Chem. Commun.* **1975**, 338–340.
(37) LaMar, G. N.; Viscio, D. B.; Smith, K. M.; Caughey, W. S.; Smith, M. L. *J. Am. Chem. Soc.* **1978**, *100*, 8085–8092.

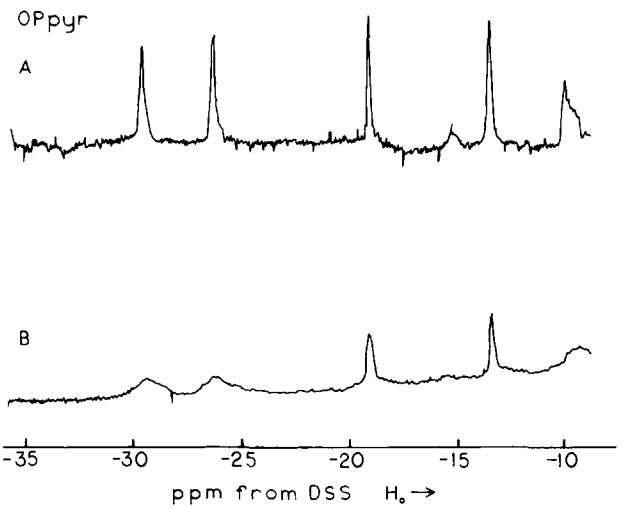

Figure 8. 100 MHz ^1H NMR spectra of 0.005 M OPpyr in D_2O at 22 °C (A) in the absence of Gd^{3+} and (B) with 5.4×10^{-4} M $GdCl_3$.

Table I. Fractional Height of Heme Methyl Group Peaks with Added Gd^{3+}

	δ (ppm from DSS)	peak height with ~5×10^{-4} M Gd^{3+} [b]	assignment
OPCN[a]	−26.66	0.17	5- or 8-methyl
	−21.63	0.28	8- or 5-methyl
	−13.85	0.44	1-methyl
	−14.30	0.53	3-methyl
OPpyr[a]	−29.97	0.19	5- or 8-methyl
	−27.07	0.17	8- or 5-methyl
	−19.35	0.40	1-methyl
	−13.45	0.49	3-methyl

[a] ~0.005 M OPCN and OPpyr. [b] Peak height expressed as the fraction of the height in the absence of Gd^{3+}.

and therefore are assigned to the 5- and 8-methyl groups. The change in line width is smallest for the furthest upfield methyl peak thus identifying it as the 3-methyl group. Figure 9 shows the change in methyl group line widths for OPCN as a function of Gd^{3+} concentration, Table I lists the fractional height of the methyl peaks at the maximum Gd^{3+} concentration, which provides a more quantitative estimate of the relative broadening.[36] The meso protons upfield of DSS also broadened out, but poor resolution prevented assignment of these peaks to individual meso protons. At lower concentrations of OPCN (~10^{-5} M) the propionic acid side chains could not compete effectively with water for Gd^{3+}, The assignments of OPCN and OPpyr methyl group resonances were only possible at higher concentrations where dimers are present. As noted above, this aggregation had only a small effect on the actual resonance positions.

Unfortunately the methyl groups of the azide and *N*-acetyl-DL-methionine complexes could not be assigned by using Gd^{3+} as a relaxation probe. The excess ligand is present to ensure complete formation of the complex coordinates to Gd^{3+}, preventing coordination to the propionic acid side chains. Integration of OPMET hyperfine shifted resonances showed that the peak at 27 ppm is due to two protons while the others arise from three protons and were therefore assigned as heme methyl resonances.

In addition to differences in the observed heme methyl group resonance positions in the ^1H BNR spectra, a marked contrast in line widths for cytochrome *c* and OPMET is apparent. Presumably the ~400 Hz line widths of OPMET methyl groups are due to rapid exchange between bound OP and free high-spin OP. The presence of a large excess of OPMET over free OP, confirmed by the absence of high-spin OP peaks, leaves the average position of methyl group peaks essentially identical with those of pure OPMET.[54] The same effect is responsible for the OPMET spectrum lacking an upfield peak at ~25 ppm which characterizes

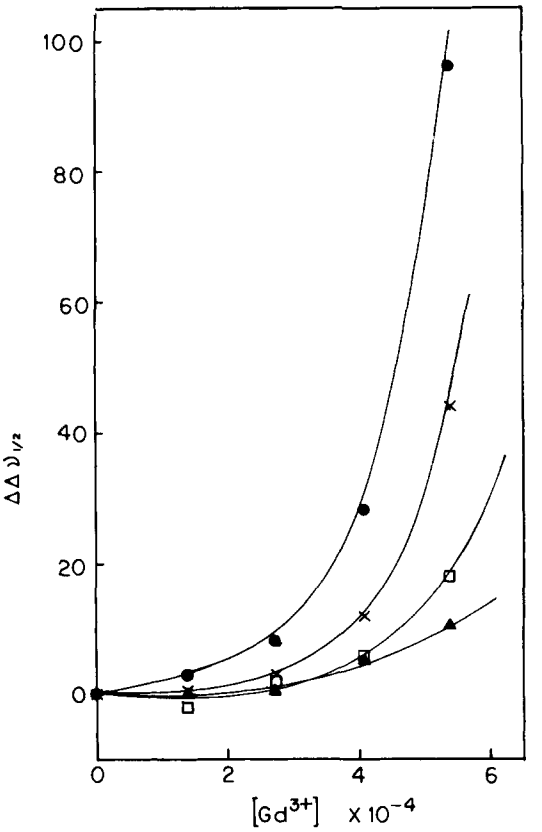

Figure 9. Change of OpCN heme methyl group line widths as a function of Gd^{3+} concentration.

methionine coordination in cytochrome *c*.[19,2] The overwhelming excess of free *N*-acetyl-DL-methionine renders the weighted average position of *N*-acetyl-DL-methionine identical with that of free *N*-acetyl-DL-methionine,

The intrinsic limitations for assigning heme methyl resonances with Gd^{3+} are as follows: at higher Gd^{3+} concentrations OP precipitates out of solution, the D_2O signal becomes too broad to function as a lock signal, and the inherent competition between water (or excess ligand) and propionic acid for Gd^{3+} restricts the concentration of OP to values where dimers are present.

Assignment of Cytochrome *c* Methyl Groups. The methyl group resonances of the azide cytochrome *c* complex have been assigned with use of saturation transfer.[5,38-40] The original saturation transfer results were reproduced and used in conjunction with the more recent methyl group assignments for cytochrome *c*[12] to make unambiguous assignments for azide cytochrome *c*.

Unfortunately the kinetics of ligand exchange for the cyanide and pyridine cytochrome *c* complexes[41] are too slow to assign methyl group resonances with saturation transfer. Apparently the spin–lattice relaxation rates for these methyl groups (with one exception) are much faster than the chemical exchange rates, The one exception appears to be the methyl group furthest downfield in the pyridine cytochrome *c* spectrum. Saturation of this methyl group was transferred to the 5-methyl group peak in cytochrome *c*, as shown in the difference spectrum of Figure 10. Since the chemical exchange rate is the same for each methyl group, the spin–lattice relaxation time of the pyridine cytochrome *c* 5-methyl group must be longer than those of the other methyl groups. The spin–lattice relaxation time for the 5-methyl group in cytochrome *c* is 75 ms compared to about 30 ms for the other methyls.[6]

An alternative method of assigning the methyl group resonances in cytochrome *c* was reported for cytochrome c_2 from *Rhodos-*

(38) Faller, J. W. In "Determination of Organic Structure by Physical Methods"; Academic Press: New York, 1975; Vol. 5, pp 75–97.
(39) Forsen, S.; Hoffman, R. A. *J. Am. Chem. Phsy.* **1963**, *39*, 2892–2901.
(40) Gupta, R. K.; Mildvan, A. S. *Methods Enzymol.* **1978**, *54*, 151–192.
(41) Sutin, J.; Yandell, J. K. *J. Biol. Chem.* **1972**, *247*, 6932–6936.

Table II. EPR Data for Cytochrome *c* and OP Derivatives

	methionine		cyanide		pyridine	
	CYTC[b]	OPMET[b]	CYTCN[c]	OPCN[c]	CYTPYR[c]	OPPYR[c]
g_1	3.04	2.92	3.26	3.28	3.29	3.29
g_2	2.25	2.29	2.01	1.97	1.99	2.06
g_3	1.28	1.51	(1.15)[d]	(1.16)[d]	1.48	1.70
$g_1^2 - 0.5(g_2^2 + g_3^2)$	5.89	4.76	7.95	8.15	7.75	7.26

[a] Abbreviations used: CYTC, cytochrome *c*; OPMET, *N*-acetyl-DL-methionine-OP; CYTCN, cyanide-cytochrome *c*; OPCN, cyanide-OP; CYTPYR, pyridine-cytochrome *c*; OPPYR, pyridine-OP. [b] Spectra obtained at 13 K in W. Orme-Johnson's lab. [c] Spectra obtained at 9 K at the National Biomedical EPR Center. [d] g_3 calculated from g_1 and g_2 as outlined in ref 53.

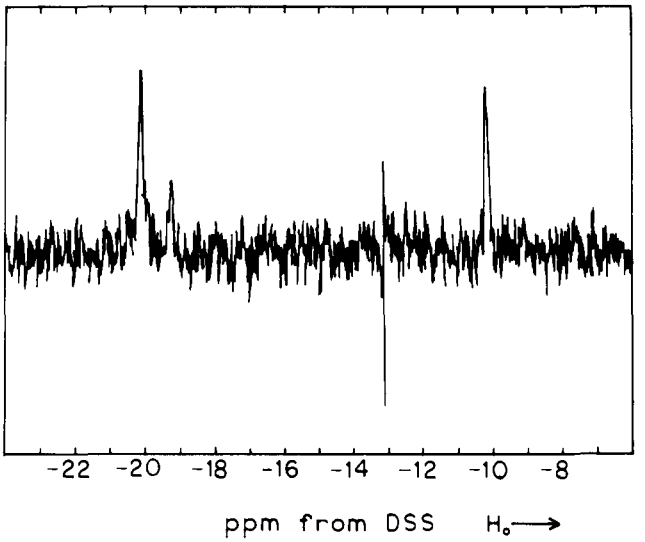

Figure 10. 400 MHz difference spectrum of a mixture of cytochrome *c* and pyridine–cytochrome *c* with saturation of pyridine–cytochrome *c* methyl group and saturation of baseline at 27 °C. Saturation is transferred to the 5-methyl group resonance of cytochrome *c*.

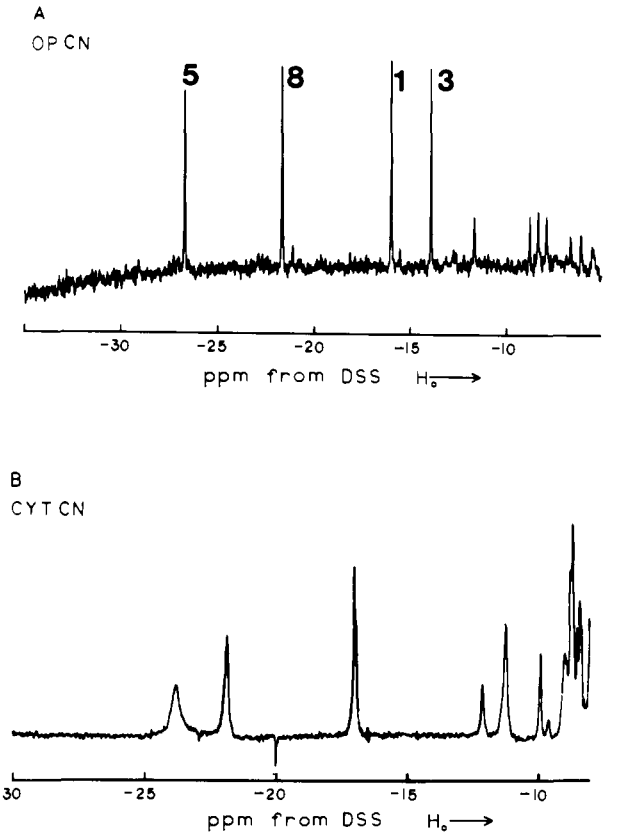

Figure 11. 400 MHz ^{1}H NMR spectra of heme methyl groups of (A) 1.6×10^{-4} M OPCN and (B) 0.002 M cyanide–cytochrome *c* in 0.05 M phosphate buffer in D_2O at 22 °C.

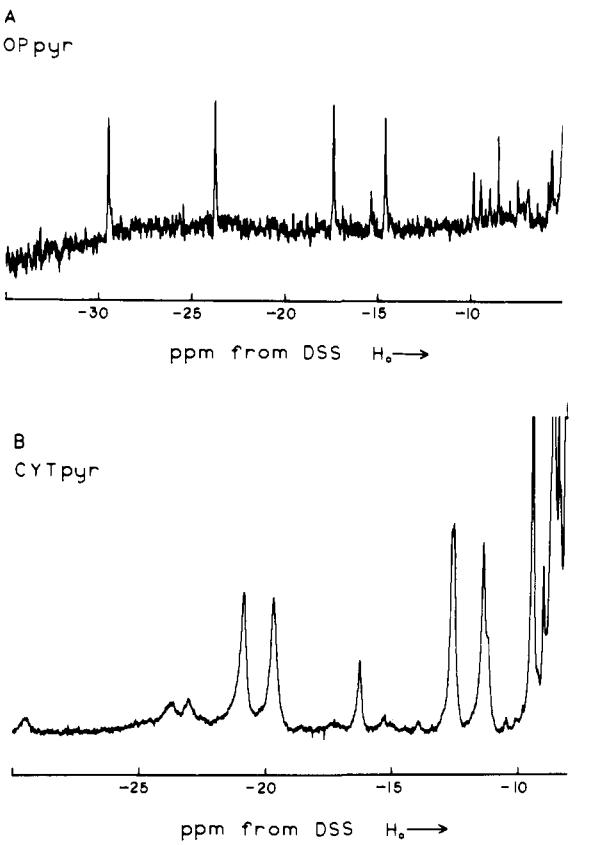

Figure 12. 400 MHz ^{1}H NMR spectra of heme methyl groups of (A) 8×10^{-5} M OPpyr and (B) ~0.004 M pyridine–cytochrome *c* in 0.05 M phosphate buffer in D_2O at 22 °C.

pirillum rubrum.[42] The solvent exposed methyl group resonance was reportedly broadened by a surface interaction with Co(phen)$_3^{2+}$, These results could not be reproduced with horse heart cytochrome *c*, which is not surprising since Co(II) is a known shift reagent not a relaxation probe.[43] A similar approach was attempted with use of Cr(phen)$_3^{3+}$ and Cr(bipy)$_3^{3+}$ as relaxation probes, These complexes did not alter the line widths of the methyl group peaks in the cytochrome *c* spectrum. This approach was abandoned since the surface interaction was not strong enough to detect,

EPR. EPR data for the cyanide,, pyridine, and *N*-acetyl-DL-methionine OP complexes and cytochrome *c* derivatives are collected in Table II. The *g* values obtained for cytochrome *c* are in excellent agreement with the literature values.[44] The cyanide cytochrome *c* *g* values differ slightly from those previously reported,[44] and the third *g* value was unresolved. Differences in experimental conditions such as solvent composition, electrolyte concentrations, excess axial ligand, and temperature may account

(42) Smith, G. M.; Kamen, M. D. *Proc. Natl. Acad. Sci. U.S.A.* **1974**, *71*, 4303–4306.
(43) Williams, R. J. P.; Moore, G. R.; Wright, P. E. In "Biological Aspects of Inorganic Chemistry", Addison, A. W., et al., Eds.; John Wiley + Sons: New York, 1977; Chapter 11.
(44) Brautigan, D. L.; Feinberg, B. A.; Hoffman, B. M.; Margoliash, E.; Peisach, J.; Blumberg, W. E. *J. Biol. Chem.* **1977**, *252*, 574–582.

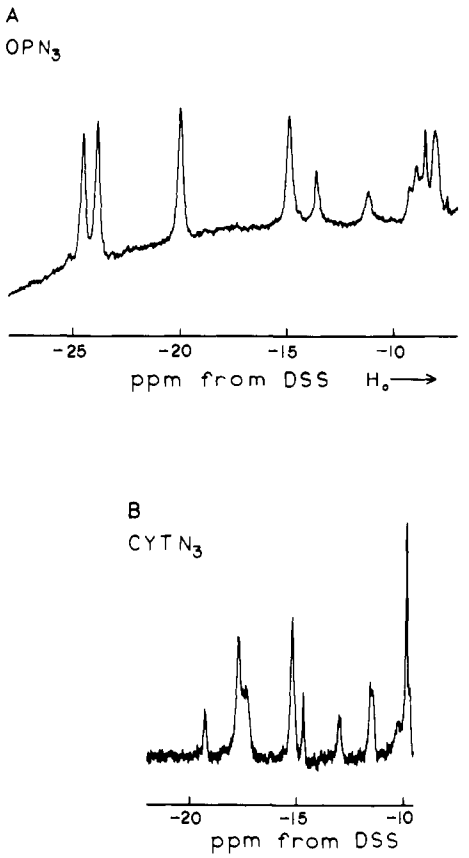

Figure 13. 400 MHz ^{1}H NMR spectra of heme methyl groups of (A) 0,001 M OPN_3 in 0.05 M phosphate buffer in D_2O with 20% CD_3OD and (B) ~0,005 M azide–cytochrome *c* in 0.05 M phosphate buffer in D_2O at 22 °C.

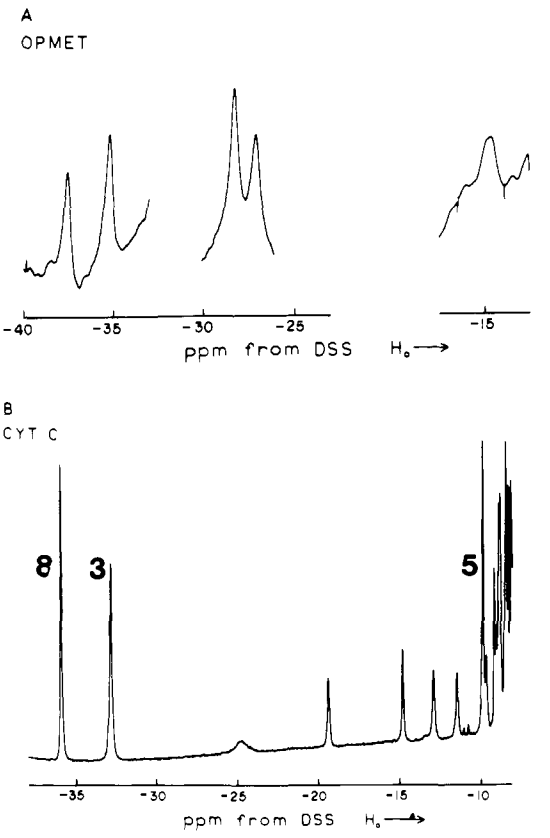

Figure 14. 400 MHz ^{1}H NMR spectra of heme methyl groups of (A) ~6×10^{-5} M OP-*N*-acetyl-DL-methionine in D_2O "pH" ~7.0 and (B) ~0.005 M cytochrome *c* in 0,05 M phosphate buffer in D_2O at 22 °C.

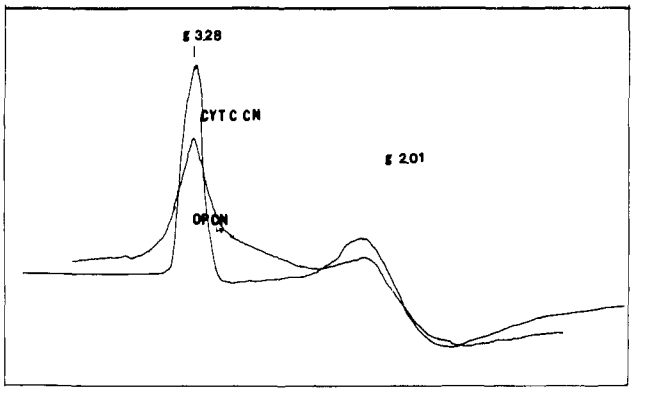

Figure 15. Comparative ESR spectra of cyano cytochrome and cyano octapeptide. T = 9 K.

for this discrepancy in *g* values.[45] Multiple forms of cytochrome *c* seem to be present in the pyridine cytochrome *c* spectrum, similar to those observed previously in the EPR spectrum of cytochrome *c*.[44] The heterogeneity in the EPR spectra of the OP complexes is due to aggregated free OP. The third *g* value for OPCN was not resolved,

A more rigorous analysis of the EPR spectra requires further study of the pH and concentration dependence, Nevertheless these data do show that the magnetic anisotropy, as reflected in the *g* values, is nearly identical with that of OP complexes and analogous cytochrome *c* complexes. This result is not surprising since model compounds have been used extensively by Peisach and Blumberg to identify axial ligands in heme proteins.[31] The experimental conditions for the EPR and NMR spectra reported here are identical, so the dipolar contribution to the isotropic shift was calculated from the *g* values obtained,

Dipolar Contributions to the Isotropic Shift. Several assumptions are made in the following analyses in order to compare the spin density distributions of cytochrome *c* with the octapeptide. These assumptions are listed below. A complete treatment of theory is not appropriate here, but many excellent references exist.[20,45,46,47]

The observed shift includes contributions from the analogous diamagnetic system, a dipolar shift contribution, and a contact shift contribution.[20]

$$(\Delta\nu/\nu)_{obsd} = (\Delta\nu/\nu)_{diamagnetic} + (\Delta\nu/\nu)_{dipolar} + (\Delta\nu/\nu)_{contact}$$

Subtracting the diamagnetic contributions gives the isotropic shift $(\Delta\nu/\nu)_{iso}$.

Calculation of the dipolar shift contribution from EPR *g* values assumes that second-order Zeeman effects are negligible, and that the spin system obeys the Curie law,[20,48] Finally, it is assumed that rhombic contributions to the magnetic anisotropy are averaged at room temperature[21] and that the system has axial symmetry, so that

$$(\Delta\nu/\nu)_{dip} = [\beta^2 S(S+1)/9kT](g^2\|^2 - g\perp^2)[(3\cos^2\theta - 1)/r^3]$$

This equation is most commonly used for dipolar shift calculations, given the relative ease of EPR *g* value measurements compared with rigorous single-crystal magnetic-susceptibility measurements.[45] Some rigor is lost, since pure Curie behavior may not exist, and the heme systems may be markedly rhombic, as shown by the three *g* values found here and in all other low-spin ferric hemes.[45] These problems limit the absolute accuracy of contact shift assignments, However, *comparisons* between the very similar

(45) Lamar, G, N.; Walker, F. A. In "The Porphyrins", Dolphin, D., Ed.; Academic Press: New York, 1979; Vol. IV, Chapter 2.
(46) LaMar, G. N. In "NMR of Paramagnetic Molecules", LaMar, G. N., Horrocks, W. D., Jr., Holm, R. H., Eds.; Academic Press: New York, 1973; Chapter 3.
(47) McConnell, H. M. *J. Chem. Phys.* **1956**, *24*, 764–766.
(48) Kurland, R. J.; McGarvey, B. R. *J. Magn. Reson.* **1970**, *2*, 286–301.

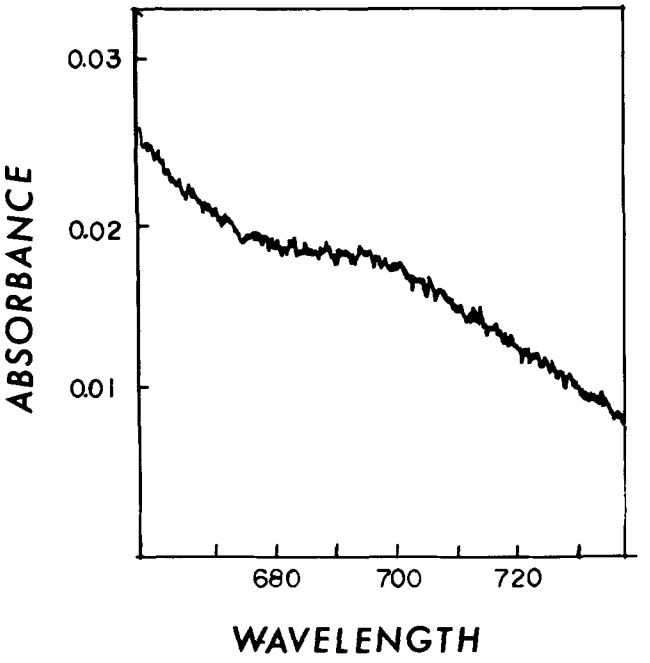

Figure 16. Visible spectrum of ~6 × 10^{-5} M OP-*N*-acetyl-DL-methionine at 22 °C.

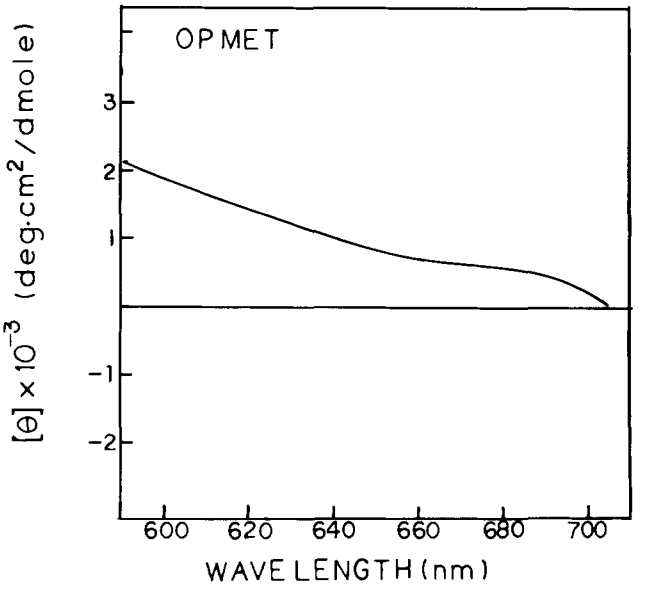

Figure 17. CD spectra of ~6 × 10^{-5} M OP-*N*-acetyl-DL-methionine at 22 °C; 5 mm path length cell.

cytochrome *c* and heme peptide samples may be made with more confidence. EPR data used for calculating dipolar shifts are compiled in Table I. The general spectral resolution can be assessed from Figure 15 which presents the EPR spectra of cyt *c* CN and OPCN.

The dipolar shifts for the model systems and protein were calculated from EPR *g* values, assuming axial symmetry. A second method for calculating dipolar shifts includes the contribution from the Rhombic term. This method is valid in the present case if the magnetic axes in the model systems and cytochrome *c* derivatives are assumed to lie on the Fe–ligand bonds, as in native cytochrome *c*[32] and other heme proteins.[34]

As shown in Figures 11–14, the hyperfine shift differences between OP complexes and cytochrome *c* complexes with the same axial ligand are substantial. The isotropic shifts, dipolar shifts, and contact shifts for these complexes are collected in Table III. The spread of isotropic shifts is larger for the OP model systems than for the analogous cytochrome *c* derivatives, This contrasts with previously reported models, which invariably have smaller isotropic shifts than the heme proteins they resemble.[18] Moreover, the large differences are due primarily to the contact shift contribution. The contact coupling constants are also reported and are directly proportional to the unpaired spin density at the pyrrole carbon.

N-Acetyl-DL-Methionine OP. The visible spectrum in Figure 16, OP-N-acetyl-DL-methionine, shows the characteristic 695-nm band of the Fe(III)–thioether bond. The CD spectrum in the same region (Figure 17) has been shown to reflect the chirality of this bond.[49] The molar eilipticity for this complex does not resemble that of horse or *Pseudomonas aeruginosa* cytochrome *c*. The orientation of the *N*-acetyl-DL-methionine is expected to be random. The slight positive ellipticity in this region may be the tail of a larger positive Cotton effect, rather than a reflection of the chirality of the iron–thioether bond.

Discussion

Magnetic Properties of OPL. As observed in previous studies with the heme peptides, aggregation effects are common.[28-30] Self-association was also apparent in the present study but was minimized by the addition of axial ligands, lowering the concentration, and in one case adding methanol to disperse the aggregates. As noted in the results section, aggregation had only a small effect on the observed methyl group resonance positions.

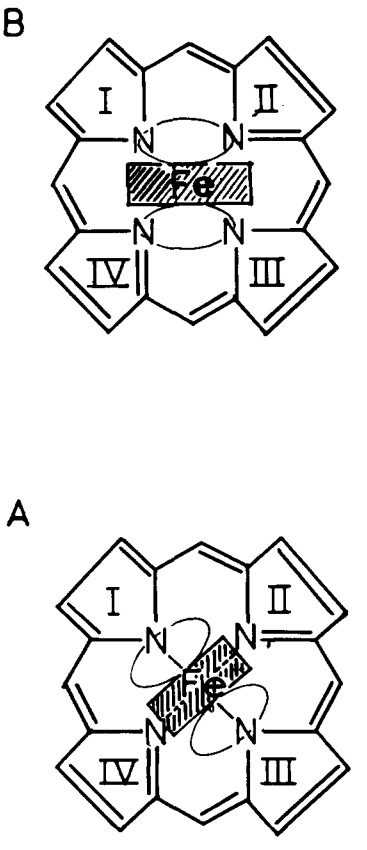

Figure 18. Possible imidazole orientations in heme proteins: (A) degeneracy of dπ orbitals lifted and (B) degeneracy of dπ orbitals not lifted.

The downfield methyl group contact shifts in the OP complexes signify a ligand-to-metal charge-transfer mechanism of electron spin density delocalization through the prophyrin π orbital, as in other low-spin Fe(III) porphyrins.[45] The upfield isotropic shifts of the OPCN and OPpyr meso protons are characteristic of the filled π prophyrin orbital transferring spin density to the metal.

The assigned methyl group resonances in the cyanide and pyridine OP complexes demonstrate that the orientation of the histidyl imidazole in OP is almost certainly the same as in cy-

(49) Senn, H.; Keller, R. M.; Wüthrich, K. *Biochem. Biophys. Res. Commun.* **1980**, *92*, 1362–1369.
(50) Cotton, F. A.; Wilkinson, G. In "Advanced Inorganic Chemistry"; John Wiley + Sons: New York, 1972; Chapter 20.

Table III. Heme Methyl Group Isotropic,[b] Dipolar, and Contact Shifts for Cytochrome c and OP Derivatives at 22 °C[a]

isotropic shift	dipolar shift	contact shift	A/h (10^{-5} Hz)
		CYTCN	
−19.53 (5)	7.58	−27.11	10.14
−17.50 (8)	3.10	−20.60	7.71
−12.94 (1)	7.58	−20.52	7.68
−7.72 (3)	3.10	−10.82	4.05
		spread 16.29	$\Sigma A/h$ = 29.60
		av −19.76	
		OPCN	
−23.06 (5, 8)	7.57	−30.63	11.46
−18.03 (8, 5)	3.38	−21.41	8.01
−22.33 (1)	7.57	−19.90	7.44
−10.25 (3)	3.38	−13.63	5.10
		spread 17.00	$\Sigma A/h$ = 32.01
		av 21.39	
		CYTC	
−33.74 (8)[c]	1.13	−34.87	13.05
−28.94 (3)[c]	1.13	−30.07	11.25
−6.49 (5)[c]	6.78	−13.27	4.96
−3.66 (1)[c]	6.78	−10.44	3.91
		spread 24.43	$\Sigma A/h$ = 33.17
		av −22.17	
		OPMET	
−34.03 (5)	5.64	−39.67	14.84
−31.65 (8)	0.75	−32.40	12.12
−24.68 (1)	5.64	−30.32	11.34
−11.28 (3)	0.75	−12.03	4.50
		spread 27.64	$\Sigma A/h$ = 42.80
		av −28.61	
		CYTPYR	
−16.95 (5)	6.67	−23.67	8.86
−15.90 (8)	3.74	−19.64	7.35
−8.90 (1)	6.67	−15.57	5.82
−7.68 (3)	3.74	−11.42	4.27
		spread 12.25	$\Sigma A/h$ = 26.30
		av −17.56	
		OPPYR	
−25.94 (5, 8)	5.99	−31.93	11.95
−20.22 (8, 5)	3.76	−23.98	8.97
−13.80 (1)	5.99	−19.79	7.40
−11.01 (3)	3.76	−14.77	5.59
		spread 17.16	$\Sigma A/h$ = 33.91
		av −22.62	
		$CYTN_3$	
−13.70 (5)	3.99[d]	−17.69	6.62 (5)
−13.33 (8)	0.64[d]	−13.97	5.23 (1)
−11.20 (1)	3.99[d]	−15.19	5.68 (8)
			$\Sigma A/h$ = 17.53 (3)
		OPN_3	
−20.90			
−20.30			
−16.40			
−11.30			

[a] Abbreviations used are the same as in Table II. Methyl group assignments given in parentheses. [b] Isotropic shifts for OP and cytochrome c derivatives calculated by subtracting −3.6 ppm from the observed shift as in ref 37. [c] Experimentally determined diamagnetic shift values used to calculate the isotropic shifts.[12] [d] Reported EPR g values (g_1 = 2.73, g_2 = 2.24, and g_3 = 1.73) were used to calculate dipolar shifts.[44]

tochrome c, In myoglobin and hemoglobin, the imidazole is close to the orientation shown in Figure 18A. The pπ orbital of imidazole has the correct symmetry to interact with the d_{xz} orbital, and thus raise its energy. Since the unpaired electron resides in the highest energy dπ orbital, lifting the degeneracy of the d orbitals also affects the interaction with the porphyrin π orbital. The maximum unpaired spin density is therefore directed toward the pyrrole rings perpendicular to the imidazole plane, Because of this symmetry-breaking perturbation the 5- and 1-methyl groups are furthest downfield in cyanomyoglobin and the 8 and 3 furthest upfield, as expected.[11,21] The imidazole orientation in cytochrome c bisects the iron pyrrole bonds as shown in Figure 18B, The pπ imidazole orbitals can interact equally with both d_{xz} and d_{yz} orbitals so the degeneracy should not be lifted, If the orientation of the imidazole were different in OP than in cytochrome c, then a pattern similar to MbCN should be observed. Either the 1- or 3-methyl group would be one of the furthest downfield methyl resonances. Instead both 1 and 3 are the furthest upfield resonances in all OP complexes with assigned methyl group resonances, Therefore, the degeneracy of the dπ orbital is not lifted by imidazole in OP, A space filling model of the octapeptide also shows that the imidazole plane orientation is the same as that in the protein.[51] and that rotation about the iron–imidazole bond is impossible.

The 2,4 substituents in OP are found to be more electron withdrawing than the propionic acid side chains since the 1- and 3-methyl groups on those pyrrole rings are shifted further upfield than the 5 and 8 groups. The L→M charge-transfer interaction responsible for transferring electron spin density is less favorable on pyrrole rings with electron-withdrawing substituents.[37]

Although the Gd^{3+} relaxation probe cannot distinguish between the 5- and 8-methyl resonances, a comparison with other porphyrin systems suggests the 5-methyl is further downfield than the 8,[37] Since the OP histidyl imidazole does not have a symmetry-breaking effect, OPCN should resemble other dicyano natural porphyrins. The only other porphyrin which has the 1- and 3-methyl groups furthest upfield in that order is the unsymmetrically substituted 4-acetyldeuteroporphyrin.[37] In this case the 5-methyl group is further downfield than the 8-methyl peak. The methyl group peaks of azido–cytochrome c also follow the 5, 8, 1, 3 pattern on going to higher fields,

The methyl group shifts in the cytochrome c derivatives almost certainly follow the same pattern as the OP analogues, The azide–cytochrome c complex has this characteristic 5, 8, 1, 3 pattern and the furthest downfield methyl group in the pyridine cytochrome c system is the 5 position. From the known orientation of imidazole in cytochrome c[52] the 8, 1, and 3 methyl groups are expected to follow in that order going upfield. This implies that pyridine does not have a preferred orientation which could split dπ orbital degeneracy.

Comparison of the OP Model and the Protein. The results of the present study illustrate that the orientation of axial ligands and heme group protein contacts can have a large influence on the electronic structure of heme c in cytochrome c, Other important symmetry-breaking perturbations, such as the 2,4 substituents, imidazole orientation, and axial ligand, were the same in the model system and protein.

The pyridine complexes of OP and cytochrome c exhibited the largest difference in contact shifts, The sum of the contact coupling constants reflects the total amount of unpaired spin density distributed to the pyrrole rings, Comparison of these total contact coupling constants shows a 27% increase in the amount of unpaired spin density at the pyrrole rings in OPpyr over pyridine cytochrome c.

The cyanide derivatives have a less pronounced difference in contact shifts. The overall increase in spin density at the pyrrole rings in OPCN is only 6%. This is probably within experimental error considering the assumptions used to derive the contact coupling constants.

Although EPR data were not obtained for the azide derivatives, the magnetic anisotropy is probably very similar for OPN_3 and

(51) Fiechtner, M. D., personal communication.
(52) Swanson, R.; Trus, B. L.; Mandel, N.; Mandel, G.; Kallai, O. B.; Dickerson, R. E. *J. Biol. Chem.* **1977**, *252*, 759–775.
(53) Palmer, G. In "The Porphyrins", Dolphin, D., Ed.; Academic Press: New York, 1979; Vol. IV, Chapter 6.
(54) Wüthrich, K. In "NMR in Biological Research: Peptides and Proteins"; American Elsevier: New York, 1976.

azido-cytochrome c as with all other derivatives. Using the reported g values for azido-cytochrome c[44] to calculate the dipolar shift, an overall 40% increase in total spin density is estimated for OPN_3.

The N-acetyl-DL-methionine-OP complex differs in dipolar shift as well as contact shift from cytochrome c. Nevertheless there is a 29% increase in overall spin density in the model as compared to cytochrome c.

This analysis demonstrates that the actual amount of increased electron spin density in the model over the protein is highly dependent on the axial ligand. Part of this dependence may be due to changes in tertiary structure of the protein from steric interactions with bulky ligands like pyridine. The heme-protein contacts would be more important for such bulky ligands. Cyanide, a smaller ligand, probably perturbs the tertiary protein structure less, resulting in much smaller overall differences between the model and the protein. However, even though azide is a small ligand, the estimated differences are large. The asymmetry in spin density among the four pyrrole rings, illustrated by the range of heme methyl contact shifts, is more pronounced in cytochrome c than OPMET. This suggests that additional structural differences between the model and the protein exist which influence the spin-density distribution. Aside from the absence of protein structure in OPMET, the only other factor which is expected to be different in the model system is methionine orientation. The tertiary structure of the protein imposes a rigid methionine orientation. This restraint is absent in the model. Comparison of the CD spectra of OPMET and cytochrome c supports this concept since large differences in methionine orientation are apparent. The more asymmetric distribution of spin density in cytochrome c over OPMET is therefore associated with the specific orientation of methionine in the protein.

Although heme methyl group assignments are not available for OPMET, the pattern of shifts is probably the 5, 8, 1, 3, pattern found for all the other OP complexes, if methionine rotates freely. In cytochrome c, however, the sulfur lone pair orbital is pointed toward pyrrole ring IV as noted previously by Wüthrich. The effect of the lone pair interaction with the $d\pi$ orbitals is to direct the maximum spin density to the 8- and 3-methyl groups. In the model system, the sulfur lone pair can interact equally with both $d\pi$ orbitals as it rotates. Spin delocalization is therefore more isotropic, which results in a smaller spread of contact shifts in OPMET.

It is attractive to speculate that the protein, through heme-amino acid contacts, actually directs electron spin density to specific pyrrole rings. However, the dramatic contrast between the 8, 3, 5, 1 pattern of native cytochrome c and the 5, 8, 1, 3 pattern for the complexes reported here indicates that the orientation of methionine probably exerts the *primary* influence on electron spin distribution in native cytochrome c.

Stereochemical Analysis of γ-Replacement and γ-Elimination Processes Catalyzed by a Pyridoxal Phosphate Dependent Enzyme

Michael N. T. Chang and Christopher T. Walsh*

Contribution from the Departments of Chemistry and Biology, Massachusetts Institute of Technology, Cambridge, Massachusetts 02139. *Received December 23, 1980*

Abstract: (Z)- and (E)-[4-^{2}H]Vinylglycine samples have been synthesized and used to determine the stereochemical outcome of a pyridoxal phosphate dependent bacterial enzyme cystathionine γ-synthase. For the first time both the γ-replacement mode, vinylglycine or O-succinylhomoserine to cystathionine, and the γ-elimination mode, vinylglycine or O-succinylhomoserine to α-ketobutyrate, have been solved stereochemically. The diastereomeric [4-^{2}H]cystathionines produced enzymically in the γ-replacement mode were degraded to [4-^{2}H]homoserines, the absolute chiralities were determined, and then the compounds were succinylated. The O-succinyl[4-^{2}H]homoserines were then processed enzymically to [4-^{2}H]cystathionines enzymically, and the stereochemical course of the first half-reaction was thereby determined.

Pyridoxal-P (PLP), the coenzyme form of vitamin B_6, is a required cofactor for enzyme-mediated transformations at the α, β, and γ carbons of α-amino acids and acts to facilitate fluxes by forming stabilized substrate-carbanion equivalents.[1a,b] Amino acids substituted at both the β and γ carbons with potential leaving groups undergo either net elimination, an internal redox reaction to release leaving group and ultimately produce α-keto acid product, or net replacement to yield an amino acid product with a new β or γ substituent, respectively. Reactions at the β carbon are obviously enabled by α-carbanion equivalents. γ-Carbon eliminations or replacements, on the other hand, represent reactions at a formally unactivated carbon center and so pose more of a chemical challenge to the enzymic catalysts.

In fact, the small subset of the pyridoxal-P-linked enzymes that act at the γ carbon of amino acid substrates first make stabilized α-carbanion equivalents then β-carbanion equivalents for anchimeric assistance to γ-substituent departure and so abstract two substrate hydrogens (C_α, C_β).[2] This process yields a fully conjugated intermediate (eq 1a of Scheme I) that has the ambident reactivity at the γ carbon to serve as common precursor to both elimination and replacement products (eq 1b) in the second half-reactions. The elimination sequence i involves reaction of C_4 (γ) of substrate equivalent as nucleophile toward a proton, hydrolytic release of the enamine, and ketonization; the replacement sequence ii features attack of an incoming cosubstrate nucleophile, y', on C_4 as the electrophilic center, followed by stereo- and regiospecific protonation at C_3 (β) then C_2 (α) carbons to unravel the intermediate to the product amino acid.

While the stereochemical outcome of various enzymatic β replacements and β eliminations have been detailed in the last few years,[3] no analysis of the more complex and difficult γ-elimination

(1) (a) Snell, E., Dimari, S. In "The Enzymes", 3rd ed.; Boyer, P., Ed.; Academic Press: New York, 1970; Vol. 2, p 335. (b) Walsh, C. In "Enzyme Reaction Mechanisms"; W. H. Freeman: San Francisco, 1979; Chapter 24.

(2) Davies, L.; Metzler, D. In "The Enzymes", 3rd ed.; Boyer, P., Ed.; Academic Press: New York, 1972; Vol. 17, p 42.

0002-7863/81/1503-4921$01.25/0